Stem Cell Reports
Article

ISSCR

OPEN ACCESS

# Atypical PKC-iota Controls Stem Cell Expansion via Regulation of the Notch Pathway

In Kyoung Mah,[1] Rachel Soloff,[2,3] Stephen M. Hedrick,[2] and Francesca V. Mariani[1,*]
[1]Broad CIRM Center for Regenerative Medicine and Stem Cell Research, Keck School of Medicine, University of Southern California, 1425 San Pablo St., Los Angeles, CA 90033, USA
[2]Department of Biological Sciences, University of California, San Diego, La Jolla, CA 92093, USA
[3]Present address: Kyowa Hakko Kirin California, Inc., 9420 Athena Circle, La Jolla, CA 92037, USA
*Correspondence: fmariani@usc.edu
http://dx.doi.org/10.1016/j.stemcr.2015.09.021


## SUMMARY

The number of stem/progenitor cells available can profoundly impact tissue homeostasis and the response to injury or disease. Here, we propose that an atypical PKC, *Prkci*, is a key player in regulating the switch from an expansion to a differentiation/maintenance phase via regulation of Notch, thus linking the polarity pathway with the control of stem cell self-renewal. *Prkci* is known to influence symmetric cell division in invertebrates; however a definitive role in mammals has not yet emerged. Using a genetic approach, we find that loss of *Prkci* results in a marked increase in the number of various stem/progenitor cells. The mechanism used likely involves inactivation and symmetric localization of NUMB, leading to the activation of NOTCH1 and its downstream effectors. Inhibition of atypical PKCs may be useful for boosting the production of pluripotent stem cells, multipotent stem cells, or possibly even primordial germ cells by promoting the stem cell/progenitor fate.

## INTRODUCTION

The control of asymmetric versus symmetric cell division in stem and progenitor cells balances self-renewal and differentiation to mediate tissue homeostasis and repair and involves key proteins that control cell polarity. In the case of excess symmetric division, too many stem-cell-like daughter cells are generated that can lead to tumor initiation and growth. Conversely, excess asymmetric cell division can severely limit the number of cells available for homeostasis and repair (Gómez-López et al., 2014; Inaba and Yamashita, 2012). The Notch pathway has been implicated in controlling stem cell self-renewal in a number of different contexts (Hori et al., 2013). However, how cell polarity, asymmetric cell division, and the activation of determinants ultimately impinges upon the control of stem cell expansion and maintenance is not fully understood. In this study, we examine the role of an atypical protein kinase C (aPKC), PRKCi, in stem cell self-renewal and, in particular, determine whether PRKCi acts via the Notch pathway.

PKCs are serine-threonine kinases that control many basic cellular processes and are typically classified into three subgroups—conventional, novel, and the aPKCs *iota* and *zeta*, which, in contrast to the others, are not activated by diacylglyceride or calcium. The aPKC proteins are best known for being central components of an evolutionarily conserved Par3-Par6-aPKC trimeric complex that controls cell polarity in *C. elegans*, *Drosophila*, *Xenopus*, zebrafish, and mammalian cells (Suzuki and Ohno, 2006).

Before Notch influences stem cell self-renewal, the regulation of cell polarity, asymmetric versus symmetric cell division, and the segregation of cell fate determinants such as NUMB may first be required (Knoblich, 2008). For example, mutational analysis in *Drosophila* has demonstrated that the aPKC-containing trimeric complex is required for maintaining polarity and for mediating asymmetric cell division during neurogenesis via activation and segregation of NUMB (Wirtz-Peitz et al., 2008). NUMB then functions as a cell fate determinant by inhibiting Notch signaling and preventing self-renewal (Wang et al., 2006). In mammals, the PAR3-PAR6-aPKC complex also can bind and phosphorylate NUMB in epithelial cells and can regulate the unequal distribution of Numb during asymmetric cell division (Smith et al., 2007). During mammalian neurogenesis, asymmetric division is also thought to involve the PAR3-PAR6-aPKC complex, NUMB segregation, and NOTCH activation (Bultje et al., 2009).

Mice deficient in *Prkcz* are grossly normal, with mild defects in secondary lymphoid organs (Leitges et al., 2001). In contrast, deficiency of the *Prkci* isozyme results in early embryonic lethality at embryonic day (E)9.5 (Seidl et al., 2013; Soloff et al., 2004). A few studies have investigated the conditional inactivation of *Prkci*; however, no dramatic changes in progenitor generation were detected in hematopoietic stem cells (HSCs) or the brain (Imai et al., 2006; Sengupta et al., 2011), although one study found evidence of a role for *Prkci* in controlling asymmetric cell division in the skin (Niessen et al., 2013). Analysis may be complicated by functional redundancy between the iota and zeta isoforms and/or because further studies perturbing aPKCs in specific cell lineages and/or at specific developmental stages are needed. Therefore, a complete picture for the

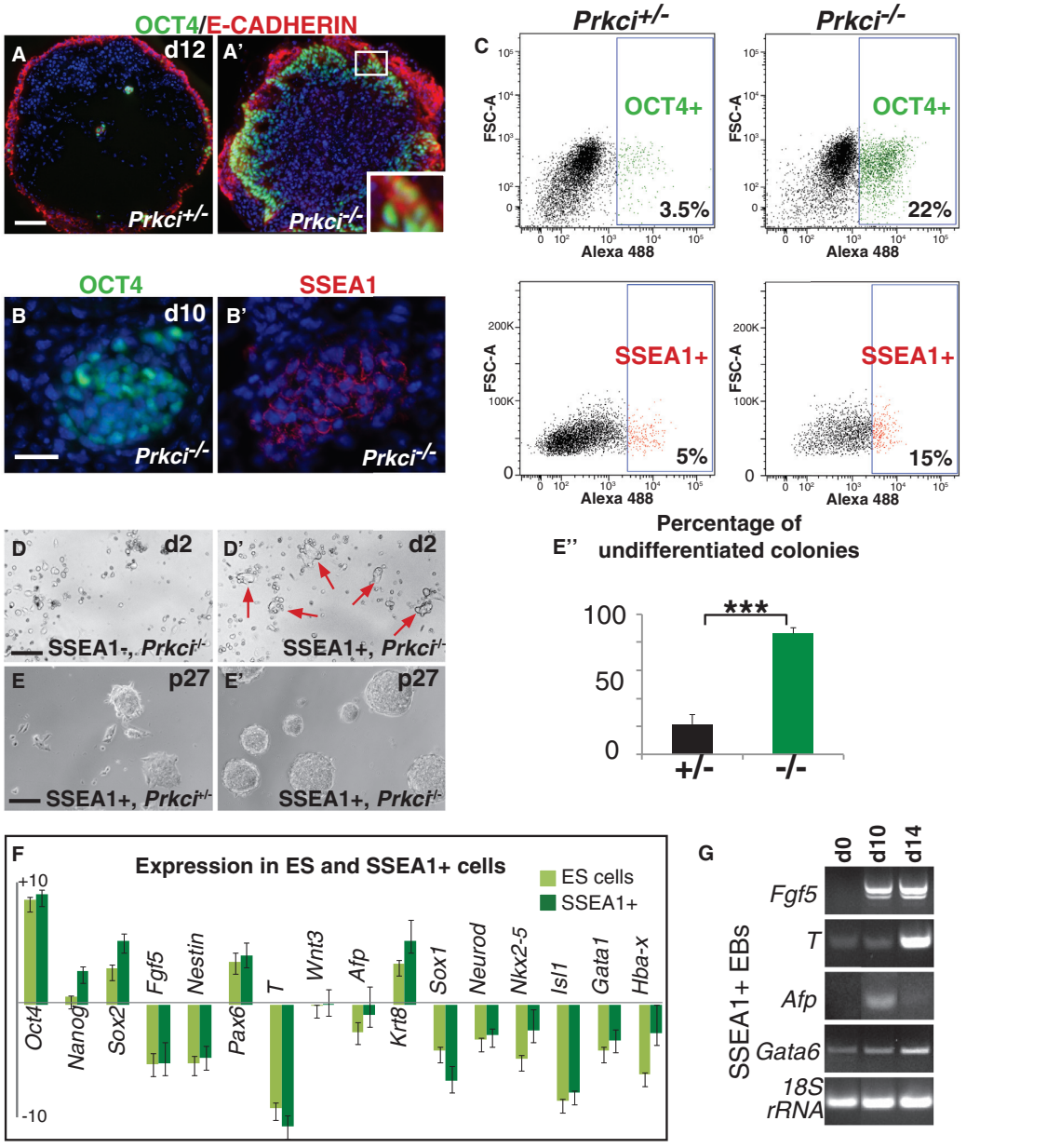


**Figure 1. *Prkci*$^{-/-}$ EBs Contain Cells with Pluripotency Characteristics**

(A and A′) Day (d) 12 heterozygous EBs have few OCT4/E-CAD+ cells, while null EBs contain many in clusters at the EB periphery. Inset: OCT4 (nucleus)/E-CAD (cytoplasm) double-positive cells.

(B and B′) Adjacent sections in a null EB show that OCT4+ cells are likely also SSEA1+.

(C) Dissociated day-12 *Prkci*$^{-/-}$ EBs contain five to six times more OCT4+ and approximately three times more SSEA1+ cells than heterozygous EBs (three independent experiments).

(D and D′) After 2 days in ES cell culture, no colonies are visible in null SSEA1− cultures while present in null SSEA1+ cultures (red arrows).

(E–E″) SSEA1+ sorted cells can be maintained for many passages, 27+. (E) *Prkci*$^{+/-}$ sorted cells make colonies with differentiated cells at the outer edges (n = 27/35). (E′) Null cells form colonies with distinct edges (n = 39/45). (E″) The percentage of undifferentiated colonies is shown. ***p < 0.001.

*(legend continued on next page)*

requirement of aPKCs at different stages of mammalian development has not yet emerged.

Here, we investigate the requirement of *Prkci* in mouse cells using an in vitro system that bypasses early embryonic lethality. Embryonic stem (ES) cells are used to make embryoid bodies (EBs) that develop like the early post-implantation embryo in terms of lineage specification and morphology and can also be maintained in culture long enough to observe advanced stages of cellular differentiation (Desbaillets et al., 2000). Using this approach, we provide genetic evidence that inactivation of *Prkci* signaling leads to enhanced generation of pluripotent cells and some types of multipotent stem cells, including cells with primordial germ cell (PGC) characteristics. In addition, we provide evidence that aPKCs ultimately regulate stem cell fate via the Notch pathway.

## RESULTS

### *Prkci*$^{-/-}$ Cultures Have More Pluripotent Cells Even under Differentiation Conditions

First, we compared *Prkci* null EB development to that of *Prkci*$^{-/-}$ embryos. Consistent with another null allele (Seidl et al., 2013), both null embryos and EBs fail to properly cavitate (Figures S1A and S1B). The failure to cavitate is unlikely to be due to the inability to form one of the three germ layers, as null EBs express germ-layer-specific genes (Figure S1E). A failure of cavitation could alternatively be caused by an accumulation of pluripotent cells. For example, EBs generated from *Timeless* knockdown cells do not cavitate and contain large numbers of OCT4-expressing cells (O'Reilly et al., 2011). In addition, EBs generated with *Prkcz* isoform knockdown cells contain OCT4+ cells under differentiation conditions (Dutta et al., 2011; Rajendran et al., 2013). Thus, we first evaluated ES colony differentiation by alkaline phosphatase (AP) staining. After 4 days without leukemia inhibitory factor (LIF), *Prkci*$^{-/-}$ ES cell colonies retained crisp boundaries and strong AP staining. In contrast, *Prkci*$^{+/-}$ colonies had uneven colony boundaries with diffuse AP staining (Figures S1F–S1F″). To definitively detect pluripotent cells, day-12 EBs were assayed for OCT4 and E-CADHERIN (E-CAD) protein expression. *Prkci*$^{+/-}$ EBs had very few OCT4/E-CAD double-positive cells (Figure 1A); however, null EBs contained large clusters of OCT4/E-CAD double-positive cells, concentrated in a peripheral zone (Figure 1A′). By examining adjacent sections, we found that OCT4+ cells could also be positive for stage-specific embryonic antigen 1 (SSEA1) (Figures 1B and 1B′). Quantification by fluorescence-activated cell sorting (FACS) analysis showed that day-12 *Prkci*$^{-/-}$ EBs had more OCT4+ and SSEA1+ cells than *Prkci*$^{+/-}$ EBs (Figure 1C). We did not find any difference between heterozygous and wild-type cells with respect to the number of OCT4+ or SSEA1+ cells or in their levels of expression for *Oct4*, *Nanog*, and *Sox2* (Figures S1I, S1I′ and S1J). However, we did find that *Oct4*, *Nanog*, and *Sox2* were highly upregulated in OCT4+ null cells (Figure S1G). Thus, together, these data indicate that *Prkci*$^{-/-}$ EBs contain large numbers of pluripotent stem cells, despite being cultured under differentiation conditions.

### Functional Pluripotency Tests

If primary EBs have a pluripotent population with the capacity to undergo self-renewal, they can easily form secondary EBs (O'Reilly et al., 2011). Using this assay, we found that more secondary EBs could be generated from *Prkci*$^{-/-}$ versus *Prkci*$^{+/-}$ EBs, especially at days 6, 10, and 16; even when plated at a low density to control for aggregation (Figure S1H). To test whether SSEA1+ cells could maintain pluripotency long term, FACS-sorted *Prkci*$^{-/-}$ SSEA1+ and SSEA1− cells were plated at a low density and maintained under ES cell culture conditions. SSEA1− cells were never able to form identifiable colonies and could not be maintained in culture (Figure 1D). SSEA1+ cells, however, formed many distinct colonies after 2 days of culture, and these cells could be maintained for over 27 passages (Figures 1D′, 1E′, and 1E″). *Prkci*$^{+/-}$ SSEA1+ cells formed colonies that easily differentiated at the outer edge, even in the presence of LIF (Figure 1E). In contrast *Prkci*$^{-/-}$ SSEA1+ cells maintained distinct round colonies (Figure 1E′). Next, we determined whether null SSEA1+ cells expressed pluripotency and differentiation markers similarly to normal ES cells. Indeed, we found that *Oct4*, *Nanog*, and *Sox2* were upregulated in both null SSEA1+ EB cells and heterozygous ES cells. In addition, differentiated markers (*Fgf5, T, Wnt3*, and *Afp*) and tissue stem/progenitor cell markers (neural: *Nestin, Sox1*, and *NeuroD*; cardiac: *Nkx2-5* and *Isl1*; and hematopoietic: *Gata1* and *Hba-x*) were downregulated in both SSEA1+ cells and heterozygous ES cells (Figure 1F). SSEA1+ cells likely have a wide range of potential, since EBs generated from these cells expressed markers for all three germ layers (Figure 1G). In addition, as expected, EBs made from null SSEA1+ cells were

(F) Sorted null cells express stem cell and differentiation markers at similar levels to normal ES cells (versus heterozygous EBs) (three independent experiments).

(G) EBs made from null SSEA1+ sorted cells express germ layer marker genes at the indicated days.

Error bars indicate mean ± SEM, three independent experiments. Scale bars, 100 μm in (A, D, and E); 25 μm in (B).

See also Figure S1.

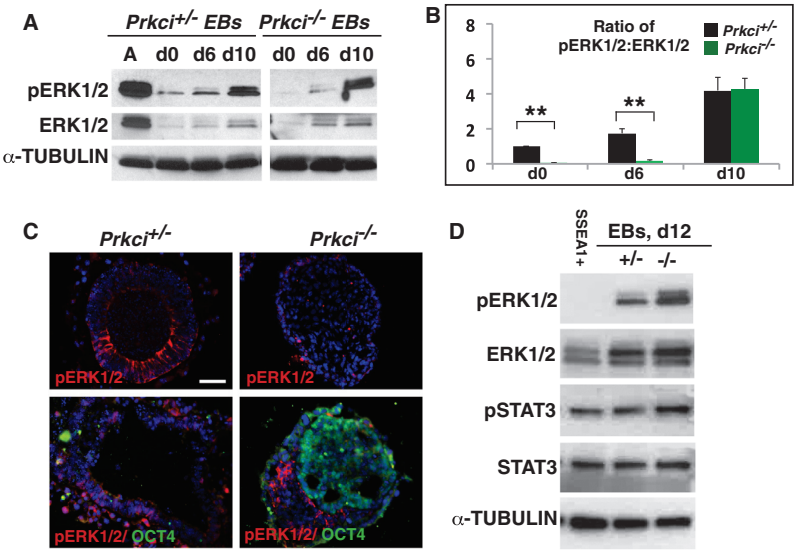


**Figure 2. *Prkci* and Pluripotency Pathways**

(A) ERK1/2 phosphorylation (Y202/Y204) is reduced in null ES cells and early day (d)-6 null EBs compared to heterozygous EBs and strongly increased at later stages. The first lane shows ES cells activated (A) by serum treatment 1 day after serum depletion.

(B) Quantification of pERK1/2 normalized to non-phosphorylated ERK1/2 (three independent experiments; mean ± SEM; $^{**}p < 0.01$).

(C) pERK1/2$^{Y202/Y204}$ is strongly expressed in the columnar epithelium of heterozygous EBs that have just cavitated. Null EBs have lower expression. OCT4 and pERK1/2 expression do not co-localize. Scale bar, 100 μm.

(D) pERK1/2$^{Y202/Y204}$ levels are lower in null SSEA1+ sorted cells than in heterozygous or in null day-12 EBs that have undergone further differentiation. pSTAT3 and STAT levels are unchanged.

See also Figure S2.

morphologically abnormal, similar to the EBs made from unsorted *Prkci*$^{-/-}$ ES cells (Figure S1G′). Thus, taken together, several assays indicate that the OCT4 and SSEA1+ populations enriched in null EBs represent pluripotent stem cells that can self-renew and have broad differentiation capacity.

## ERK1/2 Signaling during EB Development

Stem cell self-renewal has been shown to require the activation of the JAK/STAT3 and PI3K/AKT pathways and the inhibition of ERK1/2 and GSK3 pathways (Kunath et al., 2007; Niwa et al., 1998; Sato et al., 2004; Watanabe et al., 2006). We found that both STAT3 and phosphorylated STAT3 levels were not grossly altered and that the p-STAT3/STAT3 ratio was similar between heterozygous and null ES cells and EBs (Figures S2A and S2B). In addition we did not see any difference in AKT, pAKT, or β-CATENIN levels when comparing heterozygous to null ES cells or EBs (Figures S2A and S2C). Thus, the effects observed by the loss of *Prkci* are unlikely to be due to a significant alteration in the JAK/STAT3, PI3K/AKT, or GSK3 pathways.

Next, we investigated ERK1/2 expression and activation. Consistent with other studies showing ERK1/2 activation to be downstream of *Prkci* in some mammalian cell types (Boeckeler et al., 2010; Litherland et al., 2010), pERK1/2 was markedly inactivated in *Prkci* null versus heterozygous ES cells. In addition, during differentiation, null EBs displayed strong pERK1/2 inhibition early (until day 6). Later, pERK1/2 was activated strongly, as the EB began differentiating (Figures 2A and 2B). By immunofluorescence, pERK1/2 was strongly enriched in the columnar epithelium of control EBs, while overall levels were much lower in *Prkci*$^{-/-}$ EBs (Figure 2C). In addition, high OCT4 expression correlated with a marked inactivation of pERK1/2 (Figure 2C). Next, we examined *Prkci*$^{-/-}$ SSEA1+ cells by western blot. We found that SSEA1+ cells isolated from day-12 null EBs had pSTAT3 expression levels similar to whole EBs, while pERK1/2 levels were low (Figure 2D). Thus, these experiments indicate that the higher numbers of pluripotent cells in null EBs correlate with a strong inactivation of ERK1/2.

## Neural Stem Cell Fate Is Favored in *Prkci*$^{-/-}$ EBs

It is well known that ERK/MEK inhibition is not sufficient for pluripotent stem cell maintenance (Ying et al., 2008); thus, other pathways are likely involved. Therefore, we used a TaqMan Mouse Stem Cell Pluripotency Panel (#4385363) on an OpenArray platform to investigate the mechanism of *Prkci* action. Day 13 and day 20 *Prkci*$^{-/-}$ EBs expressed high levels of pluripotency and stemness markers versus heterozygous EBs, including *Oct4*, *Utf1*, *Nodal*, *Xist*, *Fgf4*, *Gal*, *Lefty1*, and *Lefty2*. However, interestingly, EBs also expressed markers for differentiated cell types and tissue stem cells, including *Sst*, *Syp*, and *Sycp3* (neural-related genes), *Isl1* (cardiac progenitor marker), *Hba-x*, and *Cd34* (hematopoietic markers). Based on this first-pass test, we sought to determine whether loss of *Prkci* might favor the generation of neural, cardiac, and hematopoietic cell types and/or their progenitors.

First, we found that null EBs contained many more NESTIN- and PAX6-positive cells than heterozygous EBs (Figures 3A and 3B; Figures S3A and S3B) (neural stem

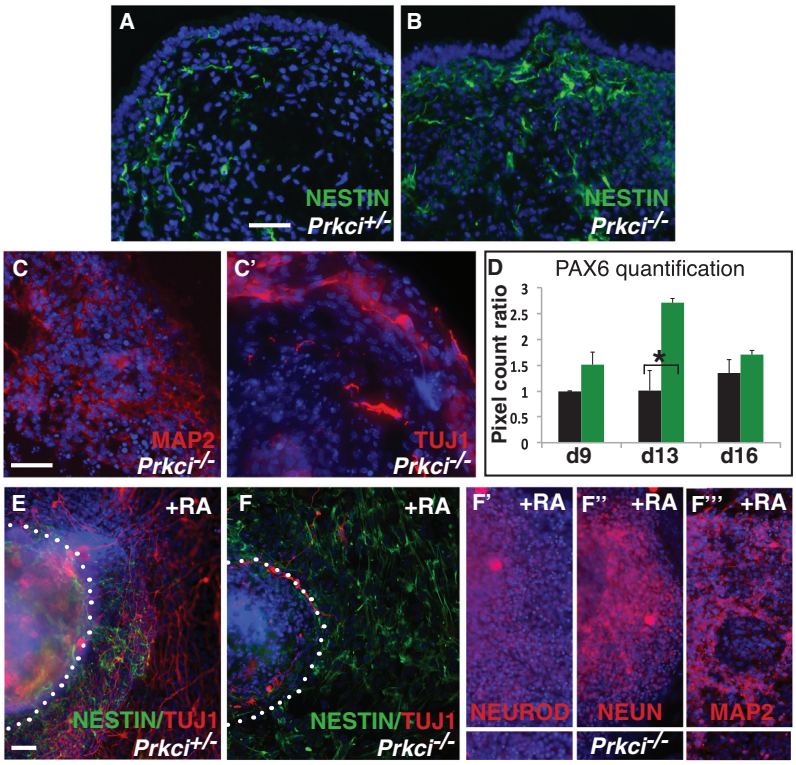


**Figure 3. Neural Stem Cell Populations Are Increased in Null EBs**

(A–C′) Prkci$^{-/-}$ EBs (B) have more NESTIN-positive cells than Prkci$^{+/-}$ EBs (A). (C and C′) MAP2 and TUJ1 are expressed in null EBs, similarly to heterozygous EBs (data not shown).

(D) EBs were assessed for PAX6 expression, and the images were used for quantification (Figures S3A and S3B). The pixel count ratio of PAX6+ cells in null EBs (green) is substantially higher than that found in heterozygous EBs (black) (three independent experiments; mean ± SEM; *p < 0.05).

(E–F‴) Day 4 after RA treatment, *Prkci*$^{-/-}$ EBs have more NESTIN- than TUJ1-positive neurons (E and F). However, null cells can still terminally differentiate into NEUROD-, NEUN-, and MAP2-positive cells (F′–F‴).

Scale bars, 25 μm in (A and C) and 50 μm in (E).

See also Figure S3.

and progenitor markers) (Sansom et al., 2009; Tohyama et al., 1992). In addition, quantification of PAX6 immunofluorescence (easier to quantify because of its nuclear localization) using a pixel count method (Fogel et al., 2012) revealed more abundant PAX6+ cells in null EBs versus heterozygous EBs. This difference was no longer evident at day 16, presumably because most of the new neural progenitors had differentiated (Figure 3D). Indeed, differentiated neuronal markers MAP2 and TUJ1 could be expressed in null cell cultures (Figures 3C and 3C′). Retinoic acid (RA) treatment both in EBs and ES cells promotes neurogenesis (Xu et al., 2012). We found that, even under RA induction, null cultures contained a larger population of NESTIN+ and a smaller population of TUJ1+ cells when compared to heterozygous cultures (Figures 3E and 3F). Again, null neural progenitors were capable of undergoing some differentiation, since we could find cells expressing NEUROD, NEUN, and MAP2 (Figures 3F′–3F‴). We also assessed neurogenesis in monolayer culture, using media that promotes neural stem cell generation supplemented with a low concentration of RA (Xu et al., 2012). Similar to the EB assay, we found that null ES cells generated a larger NESTIN+ and smaller TUJ1+ population compared to heterozygous ES cells (Figures S3C and S3D). Like in EBs, MAP2- and TUJ1-positive cells could still be found in the null cultures (Figure S3D′). Thus, using several different neural-induction assays, we found that the absence of *Prkci* correlates with the production of more neural progenitors and that, although these cells may favor self-renewal, they are still capable of progressing toward differentiation.

## The Generation of Cardiomyocyte and Erythrocyte Progenitors Is Also Favored

Next, we examined ISL1 expression (a cardiac stem cell marker) by immunofluorescence and found that *Prkci*$^{-/-}$ EBs contained larger ISL1 clusters compared with *Prkci*$^{+/-}$ EBs; this was confirmed using an image quantification assay (Figures 4A, 4A′, and 4C). Differentiated cardiac cells and ventral spinal neurons can also express ISL1 (Ericson et al., 1992); therefore, we also examined *Nkx2-5* expression, a better stem cell marker and regulator of cardiac progenitor determination (Brown et al., 2004), by RT-PCR and immunofluorescence. In null EBs, *Nkx2-5* was upregulated (Figure 4D). In addition, in response to RA, which can promote cardiac fates in vitro (Niebruegge et al., 2008), cells expressing NKX2-5 were more prevalent in null versus heterozygous EBs (Figures 4B and 4B′).The abundant cardiac progenitors found in null EBs were still capable of undergoing differentiation (Figures 4E–4F′). Indeed, more cells exhibited the striated pattern characteristic of α-ACTININ in

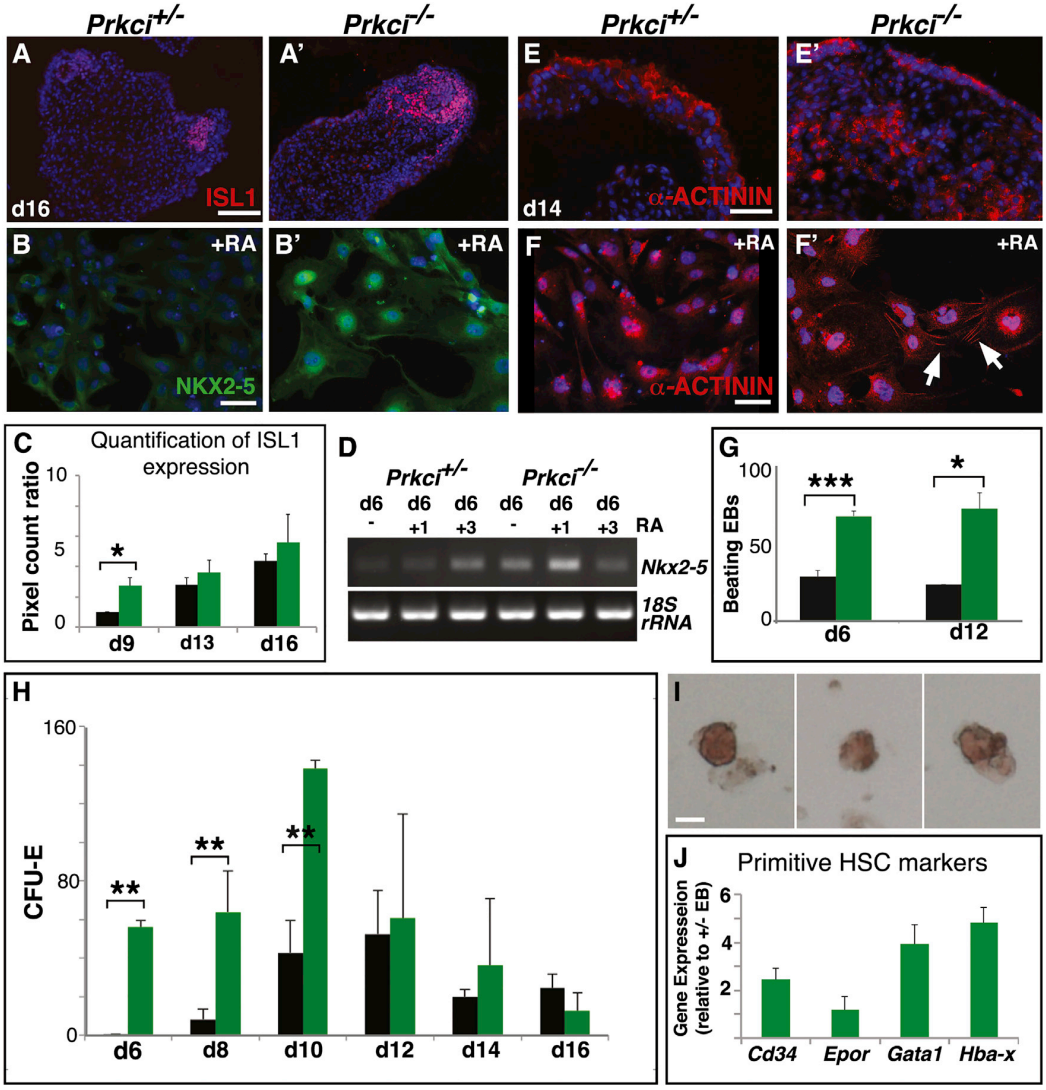


**Figure 4. Cardiomyocyte and Erythrocyte Progenitors Are Increased in *Prkci*$^{-/-}$ EBs**

(A–F′) In (A, A′, E, and E′), *Prkci*$^{-/-}$ EBs cultured without LIF have more ISL1 (cardiac progenitor marker) and α-ACTININ-positive cells compared to heterozygous EBs. (C) At day (d) 9, the pixel count ratio for ISL1 expression indicates that null EBs (green) have larger ISL1 populations than heterozygous EBs (black) (three independent experiments, n = 20 heterozygous EBs, 21 null EBs total; mean ± SEM; *p < 0.05). In (B, B′, D, F, and F′), RA treatment induces more NKX2-5 (both nuclear and cytoplasmic) and α-ACTININ expression in null EBs. Arrows point to fibers in (F′).

(G) Null EBs (green) generate more beating EBs with RA treatment compared to heterozygous EBs (black) (four independent experiments; mean ± SEM; *p < 0.05, ***p < 0.001).

(H) Dissociated null EBs of different stages (green) generate more erythrocytes in a colony-forming assay (CFU-E) (four independent experiments; mean ± SEM; **p < 0.01).

(I) Examples of red colonies.

(J) Gene expression for primitive HSC markers is upregulated in null EBs (relative to heterozygous EBs) (three independent experiments; mean ± SEM).

Scale bars, 50 μm in (A, B, and E); 100 μm in (F), and 25 μm in (I).

See also Figure S4.

null versus heterozygous EBs with RA induction (Figures 4F and 4F′). In addition, many more *Prkci*$^{-/-}$ EBs were beating after days 6 and 12 of culture (Figure 4G).

*Hba-x* expression is restricted to yolk sac blood islands and primitive erythrocyte populations (Lux et al., 2008; Trimborn et al., 1999). *Cd34* is also a primitive HSC marker (Sutherland et al., 1992). Next, we determined whether the elevated expression of these markers observed with OpenArray might represent higher numbers of primitive hematopoietic progenitors. Using a colony-forming assay (Baum et al., 1992), we found that red colonies (indicative of erythrocyte differentiation; examples in Figure 4I) were produced significantly earlier and more readily from cells isolated from null versus heterozygous EBs (Figure 4H). By quantitative real-time PCR, upregulation of *Hba-x* and *Cd34* genes confirmed the OpenArray results (Figure 4J). In addition, we found *Gata1*, an erythropoiesis-specific factor, and *Epor*, an erythropoietin receptor that mediates erythroid cell proliferation and differentiation (Chiba et al., 1991), to be highly upregulated in null versus heterozygous EBs (Figure 4J). These data suggest that the loss of *Prkci* promotes the generation of primitive erythroid progenitors that can differentiate into erythrocytes.

To determine whether the aforementioned tissue stem cells identified were represented in the OCT4+ population that we described earlier, we examined the expression of PAX6, ISL1, and OCT4 in adjacent EB sections. We found that cells expressing OCT4 appeared to represent a distinct population from those expressing PAX6 and ISL1 (although some cells were PAX6 and ISL1 double-positive) (Figures S4A–S4C).

### *Prkci*$^{-/-}$ Cells Are More Likely to Inherit NUMB/aNOTCH1 Symmetrically

The enhanced production of both pluripotent and tissue stem cells suggests that the mechanism underlying the action of *Prkci* in these different contexts is fundamentally similar. Because the Notch pathway controls stem cell self-renewal in many contexts (Hori et al., 2013), and because previous studies implicated a connection between PRKCi function and the Notch pathway (Bultje et al., 2009; Smith et al., 2007), we examined the localization and activation of a key player in the Notch pathway, NUMB, (Inaba and Yamashita, 2012). Differences in NUMB expression were first evident in whole EBs, where polarized expression was evident in the ectodermal and endodermal epithelia of heterozygous EBs, while *Prkci*$^{-/-}$ EBs exhibited a more even distribution (Figures 5A–5B′). To more definitively determine the inheritance of NUMB during cell division, doublets undergoing telophase or cytokinesis were scored for symmetric (evenly distributed in both cells) or asymmetric (unequally distributed) NUMB localization (examples: Figures 5C and 5C′). In dissociated day-10 EBs, *Prkci*$^{+/-}$ doublets displayed somewhat less symmetric versus asymmetric inheritance, while *Prkci*$^{-/-}$ doublets exhibited nearly four times more symmetric versus asymmetric inheritance (Figure 5D). Although individual cells from null EBs that were OCT4+ or PAX6+ more likely to exhibit non-polarized NUMB distribution (Figures S5A and S5B), we decided to use an assay that allowed for FACS purification, followed by the more stringent doublet assay. Therefore, we chose CD24 (heat-stable antigen; BA-1), a cell-surface marker that is highly expressed in pre-differentiated neurons and neuroblasts (Pruszak et al., 2009), and tested this marker as a method to enrich for cells destined to differentiate into neurons (see Supplemental Experimental Procedures). To assess NUMB localization, FACS-sorted CD24 cells isolated from the RA-treated EBs were then put in culture for 24 hr, and doublets were scored. Both *Prkci*$^{-/-}$ CD24$^{high}$ and CD24$^{low}$ doublets exhibited more symmetric versus asymmetric NUMB localization when compared to *Prkci*$^{+/-}$ doublets (Figure 5E) (>2× more was observed for CD24$^{low}$ doublets; 1.5 ± 0.25 [null] versus 0.67 ± 0.2 [heterozygous]). Thus, in summary, loss of *Prkci* favors the generation of cells with symmetric NUMB distribution, even during EB differentiation. In addition, in situations where neurogenesis is stimulated (RA treatment), loss of *Prkci* favors symmetric NUMB distribution in both the CD24$^{high/low}$ subpopulations.

Because NUMB can be directly phosphorylated by aPKCs (both PRKCi and PRKCz) (Smith et al., 2007; Zhou et al., 2011), loss of *Prkci* might be expected to lead to decreased NUMB phosphorylation. Three NUMB phosphorylation sites—Ser7, Ser276, and Ser295—could be aPKC mediated (Smith et al., 2007). By immunofluorescence, we found that one of the most well-characterized sites (Ser276), was strongly inactivated in null versus heterozygous EBs, especially in the core (Figures 5F and 5G). Western analysis also confirmed that the levels of pNUMB (Ser276) were decreased in null versus heterozygous EBs (Figure S5F). Thus, genetic inactivation of *Prkci* leads to a marked decrease in the phosphorylation status of NUMB.

Notch pathway inhibition by NUMB has been observed in flies and mammals (Berdnik et al., 2002; French et al., 2002). Therefore, we investigated whether reduced Numb activity in *Prkci*$^{-/-}$ EBs might lead to enhanced NOTCH1 activity and the upregulation of the downstream transcriptional readouts (Meier-Stiegen et al., 2010). An overall increase in NOTCH1 activation was supported by western blot analysis showing that the level of activated NOTCH1 (aNOTCH1) was strongly increased in day 6 and day 10 null versus heterozygous EBs (Figure S5G). This was supported by immunofluorescence in EBs, where widespread strong expression of aNOTCH1 was seen in most null cells (Figures 5I and 5I′), while in heterozygous EBs, this pattern was observed only in the OCT4+ cells (Figures 5H and 5H′).

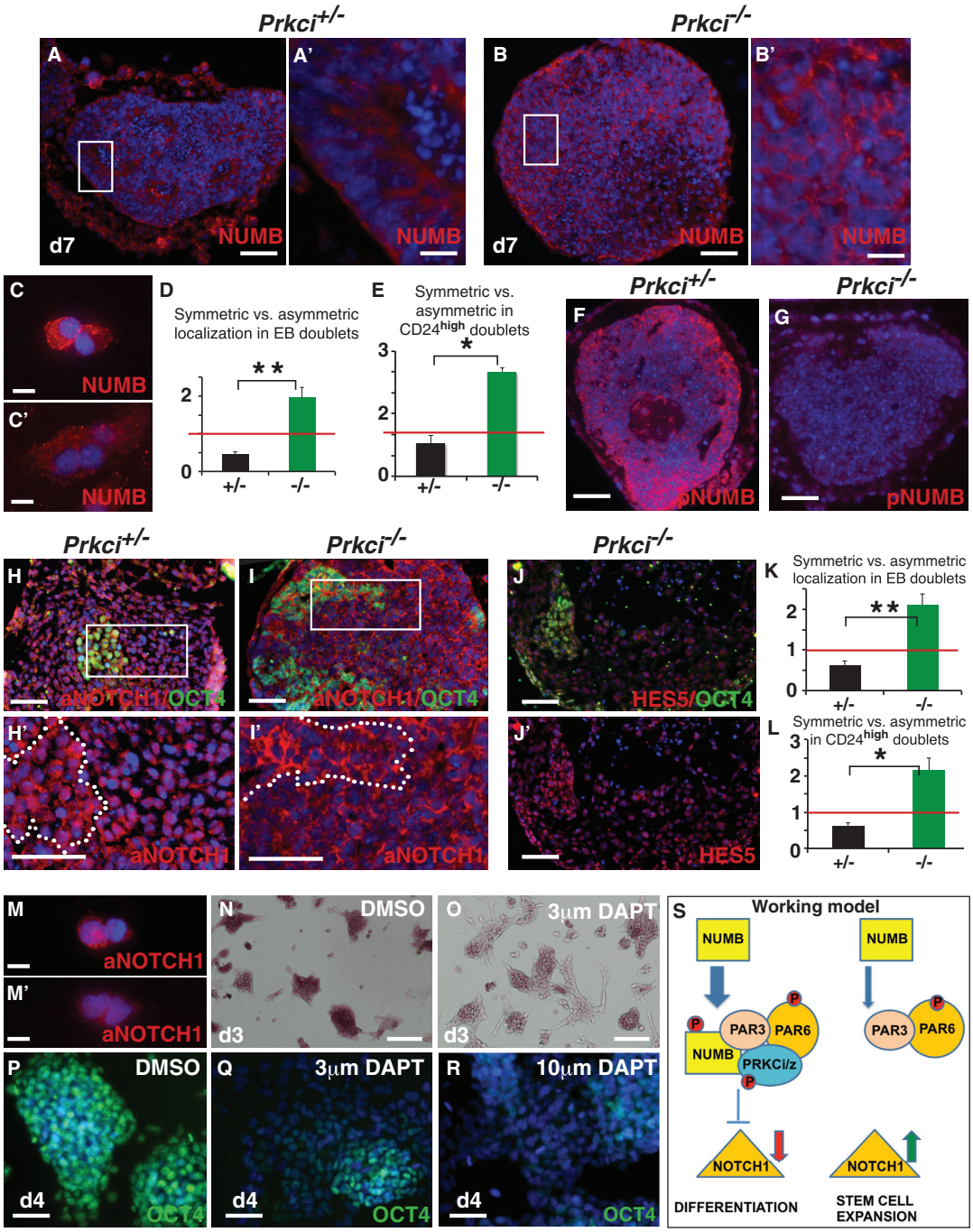


**Figure 5. *Prkci*$^{-/-}$ Cells Preferentially Inherit Symmetric Localization of NUMB and aNOTCH1 and Notch Signaling Is Required for Stem Cell Self-Renewal in Null Cells**

(A–B′) In (A and B), day (d)-7 heterozygous EBs have polarized NUMB localization within epithelia and strong expression in the endoderm, while null EBs have a more even distribution. (A′ and B′) Enlarged views.

(C and C′) Asymmetric and symmetric NUMB expression examples.

*(legend continued on next page)*

To examine the localization of aNOTCH1 and to better quantify the results seen in Figures 5H and 5I, doublets from dissociated EBs were scored. As seen with NUMB localization, null doublets were more likely to have symmetric localization of aNOTCH1 in comparison to heterozygous doublets (Figure 5K; examples in Figures 5M and 5M′). In addition, both $CD24^{high}$ and $CD24^{low}$ doublets from RA-treated null EBs were more likely to exhibit symmetric aNOTCH1 distribution versus doublets from RA-treated heterozygous EBs (Figure 5L; 3.46 ± 0.8 [null] versus 0.59 ± 0.06 [heterozygous] in $CD24^{low}$ doublets). In addition, by RT-PCR, the expression of Notch downstream genes *Hes1*, *Hes5*, *Hey1*, and *Hey2* was increased in null versus heterozygous EBs (Figure S5I). Furthermore, HES5 by immunofluorescence was broadly expressed at similar levels in both null and heterozygous cells (Figures 5J and 5J′; Figures S5H and S5H′) but more strongly expressed in null OCT4+ cells (Figures 5J and 5J′). Thus, loss of *Prkci* is associated with NOTCH1 activation, aNOTCH1 symmetric localization, and the upregulation of *Hes/Hey* downstream genes in several assays.

To determine whether Notch pathway activation is required in the absence of *Prkci*, we examined AP activity and OCT4 expression while blocking the Notch pathway using DAPT to inhibit γ-secretase (Sastre et al., 2001). DMSO-treated null ES cells stayed undifferentiated (sharp-edged colonies, strong AP staining); however, treatment of null ES cells with 3 μM DAPT led to more differentiation (AP-negative cells with cellular extensions) (Figures 5N, 5O, and S5J). In addition, OCT4 is strongly expressed in day-4 control ES cell cultures; however, in the presence of DAPT, OCT4 expression is much decreased both in monolayer culture (Figures 5P–5R) and in null EBs (48% lower OCT4+ signal versus DMSO controls, pixel counting on EB sections; data not shown). These results support the idea that activated Notch signaling is required in the absence of *Prkci* to see enhanced pluripotency.

Taken together, the combined effects of decreased NUMB activation, favored symmetric distribution of NUMB and aNOTCH1 and increased NOTCH1 activity support a model whereby loss of *Prkci* leads to sustained generation of pluripotent and some tissue stem cell populations (Figure 5S; and see Discussion).

## Additional Loss of PRKCz Activity Boosts the Number of OCT4-, SSEA1-, and STELLA-Positive Cells

The generation and maintenance of pluripotent stem cells from new sources or tissue stem cells for basic or translational research can be challenging, and there is need for new in vitro strategies. A PKC inhibitor (Gö6983) that inhibits PKCα, -β, -γ, -δ, and -ζ has been used to help maintain mouse and rat ES cells in the absence of LIF (Dutta et al., 2011; Rajendran et al., 2013). Thus, we hypothesized that treating null cells with Gö6983 might lead to better

(D) Doublets from day-10 null EBs have more symmetric inheritance when compared to day-10 heterozygous doublets (three independent experiments; mean ± SEM; **p < 0.01). A red line indicates a ratio of 1 (equal percent symmetric and asymmetric).
(E) $CD24^{high}$ null doublets exhibited more symmetric NUMB inheritance than $CD24^{high}$ heterozygous doublets (three independent experiments; mean ± SEM; *p < 0.05). A red line indicates where the ratio is 1.
(F and G) Decreased pNUMB (Ser276) is evident in the core of null versus heterozygous EBs (n = 10 of each genotype).
(H–I′) In (H and I), aNOTCH1 is strongly expressed in heterozygous EBs, including both OCT4+ and OCT4− cells, while strong aNOTCH1 expression is predominant in OCT4+ cells of null EBs (n = 10 of each genotype)). (H′ and I′) Enlarged views of boxed regions. OCT4+ cells are demarcated with dotted lines.
(J and J′) OCT4+ cells express HES5 strongly in the nucleus (three independent experiments).
(K) Null doublets from dissociated EBs have more symmetric aNOTCH1 inheritance compared to heterozygous doublets (three independent experiments; mean ± SEM; **p < 0.01). A red line indicates where the ratio is 1.
(L) $CD24^{high}$ $Prkci^{-/-}$ doublets exhibit more symmetric aNOTCH1 than $CD24^{high}$ heterozygous doublets (three independent experiments; mean ± SEM; *p < 0.05). A red line indicates where the ratio is 1.
(M and M′) Examples of asymmetric and symmetric aNOTCH1 localization.
(N and O) Day-3 DMSO-treated null ES colonies show strong AP staining all the way to the colony edge in (N). Treatment with 3 μM DAPT led to more differentiation in (O).
(P–R) OCT4 is strongly expressed in day-4 DMSO-treated null ES cultures (P). With DAPT (Q,R), OCT4 expression is decreased.
(S) Working model: In daughter cells that undergo differentiation, PRKCi can associate with PAR3 and PAR6. NUMB is recruited and directly phosphorylated. The activation of NUMB then leads to an inhibition in NOTCH1 activation and stimulation of a differentiation/maintenance program. In the absence of *Prkci*, the PAR3/PAR6 complex cannot assemble (although it may do so minimally with *Prkcz*). NUMB asymmetric localization and phosphorylation is reduced. Low levels of pNUMB are not sufficient to block NOTCH1 activation, and activated NOTCH1 preserves the stem cell self-renewal program. We suggest that PRKCi functions to drive differentiation by pushing the switch from an expansion phase that is symmetric to a differentiation and/or maintenance phase that is predominantly asymmetric. In situations of low or absent PRKCi, we propose that the expansion phase is prolonged.
Scale bars, 50 μm in (A, B, F, G, H, I, J, J′, P–R); 200 μm in (A′ and B′); 25 μm in (C, C′, M, and M′); and 100 μm in (H′, I′, N, and O).
See also Figure S5.

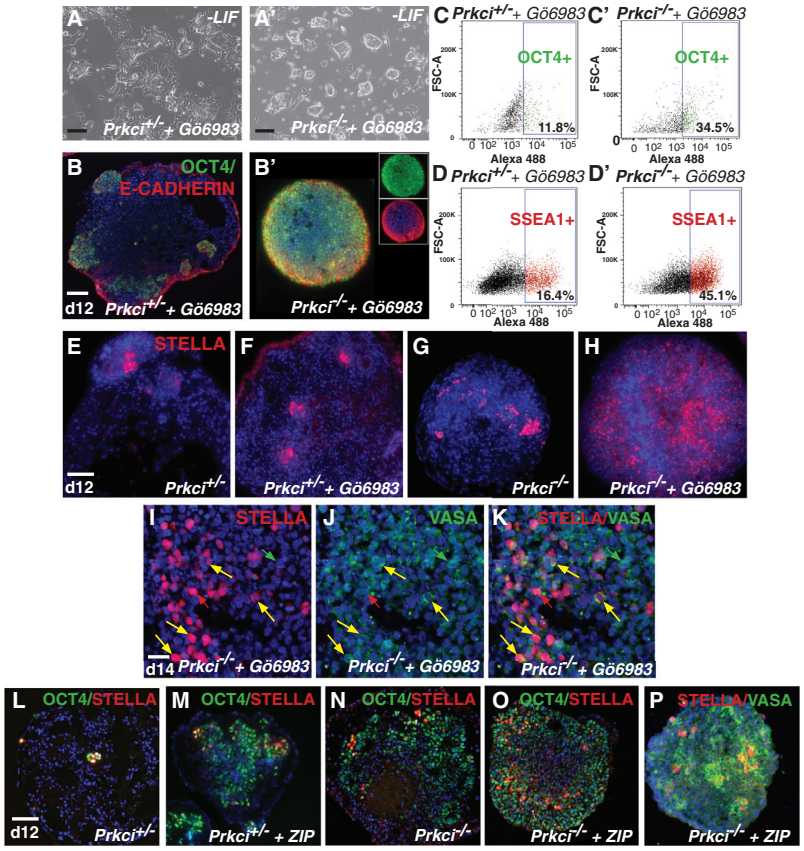


**Figure 6. Additional Inhibition of PRKCz Results in an Even Higher Percentage of OCT4-, SSEA1-, and STELLA-Positive Cells**

(A and A′) After day 4 without LIF, heterozygous ES cells undergo differentiation in the presence of Gö6983, while null ES cells stay as distinct colonies in (A′).

(B and B′) Gö6983 stimulates an increase in OCT4+ populations in heterozygous EBs and an even larger OCT4+ population in null EBs in (B′, insets: green and red channels separately).

(C–D′) An even higher percentage of cells are OCT4+ (C and C′) and SSEA1+ (D and D′) with Gö6983 treatment (day 12, three independent experiments).

(E and F) More STELLA+ clusters containing a larger number of cells are present in drug-treated heterozygous EBs.

(G and H) Null EBs also have more STELLA+ clusters and cells. Drug-treated null EBs exhibit a dramatic increase in the number of STELLA+ cells.

(I–K) Some cells are double positive for STELLA and VASA in drug-treated null EBs (yellow arrows). There are also VASA-only (green arrows) and STELLA-only cells (red arrows) (three independent experiments).

(L–P) Treatment with ZIP results in an increase in OCT4+ and STELLA+ cells. ZIP treatment also results in more cells that are VASA+ (three independent experiments); n = 11 for *Prkci*$^{+/-}$, and n = 13 for *Prkci*$^{+/-}$ + ZIP; n = 14 for *Prkci*$^{-/-}$, and n = 20 for *Prkci*$^{-/-}$ + ZIP; eight EBs assayed for both STELLA and VASA expression).

Scale bars, 100 μm in (A and A′); 50 μm in (B and B′); and 25 μm in (E, I, and L).

See also Figure S6.

stem cell expansion compared to loss of just *Prkci*. In our hands, we found that, under differentiation conditions (no LIF), heterozygous ES cells treated with the inhibitor for 4 days still underwent differentiation (Figure 6A), while treated null ES cells largely stayed undifferentiated (Figure 6A′; Figure S6A). Drug treatment of heterozygous EBs boosted the generation of OCT4-expressing cells (Figure 6B), while treatment of null EBs resulted in an even larger OCT4+ population (Figure 6B′). NUMB localization was also moderately affected (Figure S6B). By cell sorting, we found that drug treatment significantly increased the percentage of OCT4+ cells in both *Prkci*$^{+/-}$ and *Prkci*$^{-/-}$ EBs (Figures 6C and 6C′; Figures S6C and S6C′). Interestingly, Gö6983 treatment also boosted the generation of SSEA1+ cells in both null and heterozygous EBs (Figures 6D and 6D′; Figures S6D and S6D′).

SSEA1 is expressed in BLIMP1-positive PGCs derived from mouse epiblast stem cells (Hayashi and Surani, 2009). Also, PGC-like cells can be derived from isolated SSEA1+/OCT4+ EB cells (Geijsen et al., 2004). Therefore, we speculated that the increase in SSEA1 and OCT4 due to Gö6983 treatment could represent an increase in the generation of PGC-like cells instead of undifferentiated ES cells. Therefore, we examined the expression of STELLA (a PGC marker). As expected, heterozygous EBs contain small clusters of STELLA+ cells similar to EBs made of wild-type cells (Figure 6E) (Payer et al., 2006). The addition of Gö6983 to *Prkci*$^{+/-}$ EBs induced a modest increase in the number of STELLA+ cells present in the clusters (Figure 6F). Without drug treatment, null EBs contained more clusters, and the clusters contained more STELLA+ cells when compared to heterozygous EBs (Figures 6E and 6G). Interestingly, when *Prkci*$^{-/-}$ EBs were treated with Gö6983, the generation of STELLA+ cells was strongly enhanced (Figure 6G versus Figure 6H). Because undifferentiated ES cells can still express STELLA (Payer et al., 2006), we co-stained

EBs for VASA (a more differentiated PGC marker). We found many cells that were double positive (a little less than half) (Figure 6K) but also cells that expressed VASA only and STELLA only (~2× more than VASA only) (Figures 6I–6K, red/green arrows). Therefore, the combined effect of loss of *Prkci* and PKC inhibition via Gö6983 treatment leads to the production of STELLA and VASA+ PGC-like cells.

Next, we examined whether the more specific aPKC inhibitor, ZIP, a myristolated aPKC pseudosubstrate with competitive binding to p62, had similar effects (Price and Ghosh, 2013; Tsai et al., 2015; Yao et al., 2013). We found that both heterozygous and null EBs treated with ZIP contained more OCT4+ cells compared to un-treated EBs (Figures 6L–6O). In addition, like Gö6983, ZIP treatment resulted in a modest increase in the percentage of SSEA1+ cells found in heterozygous EBs and a strong increase in the percentage of SSEA1+ cells in null EBs (Figures S6E–S6F′). Furthermore, like Gö6983, both STELLA+ and VASA+ populations were increased with ZIP treatment (Figure 6P). Thus, both pluripotent and PGC-like cells can be abundantly generated with Gö6983 or ZIP treatment, suggesting that strategies that inhibit both PRKCi and/or PRKCz may be useful to maintain stem cell self-renewal and/or generate abundant PGC-like cells.

## DISCUSSION

In this report, we suggest that *Prkci* controls the balance between stem cell expansion and differentiation/maintenance by regulating the activation of NUMB, NOTCH1, and *Hes* /*Hey* downstream effector genes. In the absence of *Prkci,* the pluripotent cell fate is favored, even without LIF, yet cells still retain a broad capacity to differentiate. In addition, loss of *Prkci* results in enhanced generation of tissue progenitors such as neural stem cells and cardiomyocyte and erythrocyte progenitors. In contrast to recent findings on *Prkcz* (Dutta et al., 2011), loss of *Prkci* does not appear to influence STAT3, AKT, or GSK3 signaling but results in decreased ERK1/2 activation. We hypothesize that, in the absence of *Prkci*, although ERK1/2 inhibition may be involved, it is the decreased NUMB phosphorylation and increased NOTCH1 activation that promotes stem and progenitor cell fate. Thus, we conclude that PRKCi, a protein known to be required for cell polarity, also plays an essential role in controlling stem cell fate and generation via regulating NOTCH1 activation.

### Notch Activation Drives the Decision to Self-Renew versus Differentiate

Notch plays an important role in balancing stem cell self-renewal and differentiation in a variety of stem cell types and may be one of the key downstream effectors of *Prkci* signaling. Sustained Notch1 activity in embryonic neural progenitors has been shown to maintain their undifferentiated state (Jadhav et al., 2006). Similarly, sustained constitutive activation of NOTCH1 stimulates the proliferation of immature cardiomyocytes in the rat myocardium (Collesi et al., 2008). In HSCs, overexpression of constitutively active NOTCH1 in hematopoietic progenitors and stem cells supports both primitive and definitive HSC self-renewal (Stier et al., 2002). Together, these studies suggest that activation and/or sustained Notch signaling can lead to an increase in certain tissue stem cell populations. Thus, a working model for how tissue stem cell populations are favored in the absence of *Prkci* involves a sequence of events that ultimately leads to Notch activation. Recent studies have shown that aPKCs can be found in a complex with NUMB in both *Drosophila* and mammalian cells (Smith et al., 2007; Zhou et al., 2011); hence, in our working model (Figure 5S), we propose that the localization and phosphorylation of NUMB is highly dependent on the activity of PRKCi. When *Prkci* is downregulated or absent (as shown here), cell polarity is not promoted, leading to diffuse distribution and decreased phosphorylation of NUMB. Without active NUMB, NOTCH1 activation is enhanced, *Hes/Hey* genes are upregulated, and stem/progenitor fate generation is favored. To initiate differentiation, polarization could be stochastically determined but could also be dependent on external cues such as the presentation of certain ligands or extracellular matrix (ECM) proteins (Habib et al., 2013). When PRKCi is active and the cell becomes polarized, a trimeric complex is formed with PRKCi, PAR3, and PAR6. Numb is then recruited and phosphorylated, leading to Notch inactivation, the repression of downstream *Hes/Hey* genes, and differentiation is favored (see Figure 5S). Support for this working model comes from studies in *Drosophila* showing that the aPKC complex is essential for Numb activation and asymmetric localization (Knoblich, 2008; Smith et al., 2007; Wang et al., 2006). Additional studies on mouse neural progenitors show that regulating Numb localization and Notch activation is critical for maintaining the proper number of stem/progenitor cells in balance with differentiation (Bultje et al., 2009). Thus, an important function for PRKCi may be to regulate the switch between symmetric expansion of stem/progenitor cells to an asymmetric differentiation/maintenance phase. In situations of low or absent PRKCi, we propose that the expansion phase is favored. Thus, temporarily blocking either, or both, of the aPKC isozymes may be a powerful approach for expanding specific stem/progenitor populations for use in basic research or for therapeutic applications.

These studies, together with data presented here, provide genetic evidence that evolutionarily conserved polarity pathways may play a central role in NOTCH1 activation

and stem cell self-renewal in mammals. Further genetic studies using *Cre* transgenes that are specific for progenitors in the neural plate, primitive erythrocytes, cardiomyocytes, and other progenitors to ablate aPKC function will be needed to determine how generally this mechanism is used in diverse tissues.

Although we do not see changes in the activation status of the STAT3, AKT, or GSK3 pathway, loss of *Prkci* results in an inhibition of ERK1/2 (Figures 2A and 2B). This result is consistent with the findings that ERK1/2 inhibition is both correlated with and directly increases ES cell self-renewal (Burdon et al., 1999). Modulation of ERK1/2 activity by *Prkci* has been observed in cancer cells and chondrocytes (Litherland et al., 2010; Murray et al., 2011). Although it is not clear whether a direct interaction exists between *Prkci* and ERK1/2, *Prkcz* directly interacts with ERK1/2 in the mouse liver and in hypoxia-exposed cells (Das et al., 2008; Peng et al., 2008). The *Prkcz* isozyme is still expressed in *Prkci* null cells but evidently cannot sufficiently compensate and activate the pathway normally. Furthermore, knocking down *Prkcz* function in ES cells does not result in ERK1/2 inhibition, suggesting that this isozyme does not impact ERK1/2 signaling in ES cells (Dutta et al., 2011). Therefore, although PRKCi may interact with ERK1/2 and be directly required for its activation, ERK1/2 inhibition could also be a readout for cells that are more stem-like. Further studies will be needed to address this question.

### Utility of Inhibiting aPKC Function

Loss of *Prkci* resulted in EBs that contained slightly more STELLA+ cells than EBs made from +/− cells. Furthermore, inhibition of both aPKC isozymes by treating *Prkci* null cells with the PKC inhibitor Gö6983 or the more specific inhibitor, ZIP, strongly promoted the generation of large clusters of STELLA+ and VASA+ cells, suggesting that inhibition of both isozymes is important for PGC progenitor expansion (Figure 6). It is unclear what the mechanism for this might be; however, one possibility is that blocking both aPKCs is necessary to promote NOTCH1 activation in PGCs or in PGC progenitor cells that may ordinarily have strong inhibitions to expansion (Feng et al., 2014). Regardless of mechanism, the ability to generate PGC-like cells in culture is notoriously challenging, and our results provide a method for future studies on PGC specification and differentiation.

Expansion of stem/progenitor pools may not be desirable in the context of cancer. *Prkci* has been characterized as a human oncogene, a useful prognostic cancer marker, and a therapeutic target for cancer treatment. Overexpression of *Prkci* is found in epithelial cancers (Fields and Regala, 2007), and *Prkci* inhibitors are being evaluated as candidate cancer therapies (Atwood et al., 2013; Mansfield et al., 2013). However, because our results show that *Prkci* inhibition leads to enhanced stem cell production in vitro, *Prkci* inhibitor treatment as a cancer therapy might lead to unintended consequences (tumor overgrowth), depending on the context and treatment regimen. Thus, extending our findings to human stem and cancer stem cells is needed.

In summary, here, we demonstrate that loss of *Prkci* leads to the generation of abundant pluripotent cells, even under differentiation conditions. In addition, we show that tissue stem cells such as neural stem cells, primitive erythrocytes, and cardiomyocyte progenitors can also be abundantly produced in the absence of *Prkci*. These increases in stem cell production correlate with decreased NUMB activation and symmetric NUMB localization and require Notch signaling. Further inhibition of *Prkcz* may have an additive effect and can enhance the production of PGC-like cells. Thus, *Prkci* (along with *Prkcz*) may play key roles in stem cell self-renewal and differentiation by regulating the Notch pathway. Furthermore, inhibition of *Prkci* and or *Prkcz* activity with specific small-molecule inhibitors might be a powerful method to boost stem cell production in the context of injury or disease.

## EXPERIMENTAL PROCEDURES

### Differentiation Assays

All animal procedures were carried out in accordance with approved Animal Care and Use Protocols at the University of Southern California. *Prkci*$^{-/-}$ embryo and ES cell derivation, EB culture, and confirmation of phenotype by lentiviral transfection methods are described in the Supplemental Experimental Procedures and Figure S1. To assay neural differentiation, EBs were treated with 10 μM RA (Sigma; R2625-500MG) during days 2–6. To assay cardiomyoctye differentiation, day 6 and day 12 EBs were treated with 100 nM RA for 2 days. For the colony-forming assay, EBs were dissociated into single cells (0.25% collagenase type IV, GIBCO, 17104-019), resuspended in MethoCult GF M3434 (Stem Cell Technologies), and cultured for 2 weeks.

For DAPT treatment, ES cells were cultured for 24 hr without LIF, then for 4 days in 3 μM or 10 μM DAPT (Calbiochem, 565784) or carrier (DMSO). Samples were assayed by immunofluoresence or for alkaline phosphatase activity (Millipore, SCR004).

To inhibit aPKCs, ES cells were treated with 5 μM Gö6983 (Sigma), 20 μM of the pseudo-substrate ZIP (Anaspec, 63361 Myr-SIYRRGARRWRKL), or an equivalent amount of carrier (DMSO) and then used to make EBs, which were treated with 5 μM Gö6983 or 20 μM ZIP every other day. ZIP treatment did not affect *Prkcz* RNA or protein expression levels (Figures S6G and S6H).

Immunofluorescence and sorting assays are described in the Supplemental Experimental Procedures.

### RNA Expression

#### *Semiquantitative*

Total RNA (RNeasy Extraction Kit, QIAGEN) was reverse transcribed using M-MuLV Reverse Transcriptase (New England Biolabs,

M0253S) with random hexamers (Invitrogen, N8080127). See Table S2 for PCR primer sequences.

*RealTime Ready*

Total RNA was isolated with the High Pure RNA Isolation Kit (Roche) and reverse transcribed with the Transcriptor First Strand cDNA Synthesis Kit (Roche). PCR was carried out using the LightCycler 480 Probes Master Mix and a LightCycler 480 RealTime Ready custom plate (Roche). Unless otherwise noted, expression was normalized to the mean expression of four reference genes (*beta-actin*, *Gapdh*, *B2m*, and *Eef1a1*).

### Quantitative Analysis

The unpaired Student's t test in Microsoft Excel was used to evaluate statistical significance. For doublet analysis, data are displayed as a ratio of symmetric versus asymmetric localization, where the value 1 represents both found equally (details in Supplemental Experimental Procedures).

## SUPPLEMENTAL INFORMATION

Supplemental Information includes Supplemental Experimental Procedures, six figures, and two tables and can be found with this article online at http://dx.doi.org/10.1016/j.stemcr.2015.09.021.

## ACKNOWLEDGMENTS

We thank Sophia Tran, Audrey Izuhara, and Christy Furukawa for technical assistance and Drs. Qilong Ying, Gregor Adams, Daniel Lakeland, and Amander Clark for expertise and sharing reagents. We thank Life Technologies for assistance with OpenArray and Roche for the RealTime Ready custom plates. F.V.M. and I.K.M. were supported by USC and the Robert E. and May R. Wright Foundation. The USC Flow Cytometry Core Facility is supported in part by the National Cancer Institute (P30CA014089) and the Keck School of Medicine. The content is solely the responsibility of the authors.

Received: February 19, 2015
Revised: September 25, 2015
Accepted: September 28, 2015
Published: October 29, 2015

## REFERENCES

Atwood, S.X., Li, M., Lee, A., Tang, J.Y., and Oro, A.E. (2013). GLI activation by atypical protein kinase C ι/λ regulates the growth of basal cell carcinomas. Nature *494*, 484–488.

Baum, C.M., Weissman, I.L., Tsukamoto, A.S., Buckle, A.M., and Peault, B. (1992). Isolation of a candidate human hematopoietic stem-cell population. Proc. Natl. Acad. Sci. USA *89*, 2804–2808.

Berdnik, D., Török, T., González-Gaitán, M., and Knoblich, J.A. (2002). The endocytic protein alpha-Adaptin is required for numb-mediated asymmetric cell division in Drosophila. Dev. Cell *3*, 221–231.

Boeckeler, K., Rosse, C., Howell, M., and Parker, P.J. (2010). Manipulating signal delivery - plasma-membrane ERK activation in aPKC-dependent migration. J. Cell Sci. *123*, 2725–2732.

Brown, C.O., 3rd, Chi, X., Garcia-Gras, E., Shirai, M., Feng, X.H., and Schwartz, R.J. (2004). The cardiac determination factor, Nkx2-5, is activated by mutual cofactors GATA-4 and Smad1/4 via a novel upstream enhancer. J. Biol. Chem. *279*, 10659–10669.

Bultje, R.S., Castaneda-Castellanos, D.R., Jan, L.Y., Jan, Y.N., Kriegstein, A.R., and Shi, S.H. (2009). Mammalian Par3 regulates progenitor cell asymmetric division via notch signaling in the developing neocortex. Neuron *63*, 189–202.

Burdon, T., Stracey, C., Chambers, I., Nichols, J., and Smith, A. (1999). Suppression of SHP-2 and ERK signalling promotes self-renewal of mouse embryonic stem cells. Dev. Biol. *210*, 30–43.

Chiba, T., Ikawa, Y., and Todokoro, K. (1991). GATA-1 transactivates erythropoietin receptor gene, and erythropoietin receptor-mediated signals enhance GATA-1 gene expression. Nucleic Acids Res. *19*, 3843–3848.

Collesi, C., Zentilin, L., Sinagra, G., and Giacca, M. (2008). Notch1 signaling stimulates proliferation of immature cardiomyocytes. J. Cell Biol. *183*, 117–128.

Das, M., Burns, N., Wilson, S.J., Zawada, W.M., and Stenmark, K.R. (2008). Hypoxia exposure induces the emergence of fibroblasts lacking replication repressor signals of PKCzeta in the pulmonary artery adventitia. Cardiovasc. Res. *78*, 440–448.

Desbaillets, I., Ziegler, U., Groscurth, P., and Gassmann, M. (2000). Embryoid bodies: an in vitro model of mouse embryogenesis. Exp. Physiol. *85*, 645–651.

Dutta, D., Ray, S., Home, P., Larson, M., Wolfe, M.W., and Paul, S. (2011). Self-renewal versus lineage commitment of embryonic stem cells: protein kinase C signaling shifts the balance. Stem Cells *29*, 618–628.

Ericson, J., Thor, S., Edlund, T., Jessell, T.M., and Yamada, T. (1992). Early stages of motor neuron differentiation revealed by expression of homeobox gene Islet-1. Science *256*, 1555–1560.

Feng, Y.M., Liang, G.J., Pan, B., Qin, X.S., Zhang, X.F., Chen, C.L., Li, L., Cheng, S.F., De Felici, M., and Shen, W. (2014). Notch pathway regulates female germ cell meiosis progression and early oogenesis events in fetal mouse. Cell Cycle *13*, 782–791.

Fields, A.P., and Regala, R.P. (2007). Protein kinase C iota: human oncogene, prognostic marker and therapeutic target. Pharmacol. Res. *55*, 487–497.

Fogel, J.L., Thein, T.Z., and Mariani, F.V. (2012). Use of LysoTracker to detect programmed cell death in embryos and differentiating embryonic stem cells. J. Vis. Exp. (68), 4254.

French, M.B., Koch, U., Shaye, R.E., McGill, M.A., Dho, S.E., Guidos, C.J., and McGlade, C.J. (2002). Transgenic expression of numb inhibits notch signaling in immature thymocytes but does not alter T cell fate specification. J. Immunol. *168*, 3173–3180.

Geijsen, N., Horoschak, M., Kim, K., Gribnau, J., Eggan, K., and Daley, G.Q. (2004). Derivation of embryonic germ cells and male gametes from embryonic stem cells. Nature *427*, 148–154.

Gómez-López, S., Lerner, R.G., and Petritsch, C. (2014). Asymmetric cell division of stem and progenitor cells during homeostasis and cancer. Cell. Mol. Life Sci. *71*, 575–597.

Habib, S.J., Chen, B.C., Tsai, F.C., Anastassiadis, K., Meyer, T., Betzig, E., and Nusse, R. (2013). A localized Wnt signal orients asymmetric stem cell division in vitro. Science *339*, 1445–1448.

Hayashi, K., and Surani, M.A. (2009). Self-renewing epiblast stem cells exhibit continual delineation of germ cells with epigenetic reprogramming in vitro. Development *136*, 3549–3556.

Hori, K., Sen, A., and Artavanis-Tsakonas, S. (2013). Notch signaling at a glance. J. Cell Sci. *126*, 2135–2140.

Imai, F., Hirai, S., Akimoto, K., Koyama, H., Miyata, T., Ogawa, M., Noguchi, S., Sasaoka, T., Noda, T., and Ohno, S. (2006). Inactivation of aPKClambda results in the loss of adherens junctions in neuroepithelial cells without affecting neurogenesis in mouse neocortex. Development *133*, 1735–1744.

Inaba, M., and Yamashita, Y.M. (2012). Asymmetric stem cell division: precision for robustness. Cell Stem Cell *11*, 461–469.

Jadhav, A.P., Cho, S.H., and Cepko, C.L. (2006). Notch activity permits retinal cells to progress through multiple progenitor states and acquire a stem cell property. Proc. Natl. Acad. Sci. USA *103*, 18998–19003.

Knoblich, J.A. (2008). Mechanisms of asymmetric stem cell division. Cell *132*, 583–597.

Kunath, T., Saba-El-Leil, M.K., Almousailleakh, M., Wray, J., Meloche, S., and Smith, A. (2007). FGF stimulation of the Erk1/2 signalling cascade triggers transition of pluripotent embryonic stem cells from self-renewal to lineage commitment. Development *134*, 2895–2902.

Leitges, M., Sanz, L., Martin, P., Duran, A., Braun, U., García, J.F., Camacho, F., Diaz-Meco, M.T., Rennert, P.D., and Moscat, J. (2001). Targeted disruption of the zetaPKC gene results in the impairment of the NF-kappaB pathway. Mol. Cell *8*, 771–780.

Litherland, G.J., Elias, M.S., Hui, W., Macdonald, C.D., Catterall, J.B., Barter, M.J., Farren, M.J., Jefferson, M., and Rowan, A.D. (2010). Protein kinase C isoforms zeta and iota mediate collagenase expression and cartilage destruction via STAT3- and ERK-dependent c-fos induction. J. Biol. Chem. *285*, 22414–22425.

Lux, C.T., Yoshimoto, M., McGrath, K., Conway, S.J., Palis, J., and Yoder, M.C. (2008). All primitive and definitive hematopoietic progenitor cells emerging before E10 in the mouse embryo are products of the yolk sac. Blood *111*, 3435–3438.

Mansfield, A.S., Fields, A.P., Jatoi, A., Qi, Y., Adjei, A.A., Erlichman, C., and Molina, J.R. (2013). Phase I dose escalation study of the PKCι inhibitor aurothiomalate for advanced non-small-cell lung cancer, ovarian cancer, and pancreatic cancer. Anticancer Drugs *24*, 1079–1083.

Meier-Stiegen, F., Schwanbeck, R., Bernoth, K., Martini, S., Hieronymus, T., Ruau, D., Zenke, M., and Just, U. (2010). Activated Notch1 target genes during embryonic cell differentiation depend on the cellular context and include lineage determinants and inhibitors. PLoS ONE *5*, e11481.

Murray, N.R., Kalari, K.R., and Fields, A.P. (2011). Protein kinase Cι expression and oncogenic signaling mechanisms in cancer. J. Cell. Physiol. *226*, 879–887.

Niebruegge, S., Nehring, A., Bär, H., Schroeder, M., Zweigerdt, R., and Lehmann, J. (2008). Cardiomyocyte production in mass suspension culture: embryonic stem cells as a source for great amounts of functional cardiomyocytes. Tissue Eng. Part A *14*, 1591–1601.

Niessen, M.T., Scott, J., Zielinski, J.G., Vorhagen, S., Sotiropoulou, P.A., Blanpain, C., Leitges, M., and Niessen, C.M. (2013). aPKCλ controls epidermal homeostasis and stem cell fate through regulation of division orientation. J. Cell Biol. *202*, 887–900.

Niwa, H., Burdon, T., Chambers, I., and Smith, A. (1998). Self-renewal of pluripotent embryonic stem cells is mediated via activation of STAT3. Genes Dev. *12*, 2048–2060.

O'Reilly, L.P., Watkins, S.C., and Smithgall, T.E. (2011). An unexpected role for the clock protein timeless in developmental apoptosis. PLoS ONE *6*, e17157.

Payer, B., Chuva de Sousa Lopes, S.M., Barton, S.C., Lee, C., Saitou, M., and Surani, M.A. (2006). Generation of stella-GFP transgenic mice: a novel tool to study germ cell development. Genesis *44*, 75–83.

Peng, Y., Sigua, C.A., Rideout, D., and Murr, M.M. (2008). Deletion of toll-like receptor-4 downregulates protein kinase C-zeta and attenuates liver injury in experimental pancreatitis. Surgery *143*, 679–685.

Price, T.J., and Ghosh, S. (2013). ZIPping to pain relief: the role (or not) of PKMζ in chronic pain. Mol. Pain *9*, 6.

Pruszak, J., Ludwig, W., Blak, A., Alavian, K., and Isacson, O. (2009). CD15, CD24, and CD29 define a surface biomarker code for neural lineage differentiation of stem cells. Stem Cells *27*, 2928–2940.

Rajendran, G., Dutta, D., Hong, J., Paul, A., Saha, B., Mahato, B., Ray, S., Home, P., Ganguly, A., Weiss, M.L., and Paul, S. (2013). Inhibition of protein kinase C signaling maintains rat embryonic stem cell pluripotency. J. Biol. Chem. *288*, 24351–24362.

Sansom, S.N., Griffiths, D.S., Faedo, A., Kleinjan, D.J., Ruan, Y., Smith, J., van Heyningen, V., Rubenstein, J.L., and Livesey, F.J. (2009). The level of the transcription factor Pax6 is essential for controlling the balance between neural stem cell self-renewal and neurogenesis. PLoS Genet. *5*, e1000511.

Sastre, M., Steiner, H., Fuchs, K., Capell, A., Multhaup, G., Condron, M.M., Teplow, D.B., and Haass, C. (2001). Presenilin-dependent gamma-secretase processing of beta-amyloid precursor protein at a site corresponding to the S3 cleavage of Notch. EMBO Rep. *2*, 835–841.

Sato, N., Meijer, L., Skaltsounis, L., Greengard, P., and Brivanlou, A.H. (2004). Maintenance of pluripotency in human and mouse embryonic stem cells through activation of Wnt signaling by a pharmacological GSK-3-specific inhibitor. Nat. Med. *10*, 55–63.

Seidl, S., Braun, U., Roos, N., Li, S., Lüdtke, T.H., Kispert, A., and Leitges, M. (2013). Phenotypical analysis of atypical PKCs in vivo function display a compensatory system at mouse embryonic day 7.5. PLoS ONE *8*, e62756.

Sengupta, A., Duran, A., Ishikawa, E., Florian, M.C., Dunn, S.K., Ficker, A.M., Leitges, M., Geiger, H., Diaz-Meco, M., Moscat, J., and Cancelas, J.A. (2011). Atypical protein kinase C (aPKCzeta and aPKClambda) is dispensable for mammalian hematopoietic stem cell activity and blood formation. Proc. Natl. Acad. Sci. USA *108*, 9957–9962.

Smith, C.A., Lau, K.M., Rahmani, Z., Dho, S.E., Brothers, G., She, Y.M., Berry, D.M., Bonneil, E., Thibault, P., Schweisguth, F., et al. (2007). aPKC-mediated phosphorylation regulates asymmetric

membrane localization of the cell fate determinant Numb. EMBO J. *26*, 468–480.

Soloff, R.S., Katayama, C., Lin, M.Y., Feramisco, J.R., and Hedrick, S.M. (2004). Targeted deletion of protein kinase C lambda reveals a distribution of functions between the two atypical protein kinase C isoforms. J. Immunol. *173*, 3250–3260.

Stier, S., Cheng, T., Dombkowski, D., Carlesso, N., and Scadden, D.T. (2002). Notch1 activation increases hematopoietic stem cell self-renewal in vivo and favors lymphoid over myeloid lineage outcome. Blood *99*, 2369–2378.

Sutherland, D.R., Marsh, J.C., Davidson, J., Baker, M.A., Keating, A., and Mellors, A. (1992). Differential sensitivity of CD34 epitopes to cleavage by Pasteurella haemolytica glycoprotease: implications for purification of CD34-positive progenitor cells. Exp. Hematol. *20*, 590–599.

Suzuki, A., and Ohno, S. (2006). The PAR-aPKC system: lessons in polarity. J. Cell Sci. *119*, 979–987.

Tohyama, T., Lee, V.M., Rorke, L.B., Marvin, M., McKay, R.D., and Trojanowski, J.Q. (1992). Nestin expression in embryonic human neuroepithelium and in human neuroepithelial tumor cells. Lab. Invest. *66*, 303–313.

Trimborn, T., Gribnau, J., Grosveld, F., and Fraser, P. (1999). Mechanisms of developmental control of transcription in the murine alpha- and beta-globin loci. Genes Dev. *13*, 112–124.

Tsai, L.L., Xie, L., Dore, K., Xie, L., Del Rio, J.C., King, C.C., Martinez-Ariza, G., Hulme, C., Malinow, R., Bourne, P.E., et al. (2015). Zeta inhibitory peptide disrupts electrostatic interactions that maintain atypical protein kinase C in its active conformation on the scaffold p62. J. Biol. Chem. *290*, 21845–21856.

Wang, H., Somers, G.W., Bashirullah, A., Heberlein, U., Yu, F., and Chia, W. (2006). Aurora-A acts as a tumor suppressor and regulates self-renewal of Drosophila neuroblasts. Genes Dev. *20*, 3453–3463.

Watanabe, S., Umehara, H., Murayama, K., Okabe, M., Kimura, T., and Nakano, T. (2006). Activation of Akt signaling is sufficient to maintain pluripotency in mouse and primate embryonic stem cells. Oncogene *25*, 2697–2707.

Wirtz-Peitz, F., Nishimura, T., and Knoblich, J.A. (2008). Linking cell cycle to asymmetric division: Aurora-A phosphorylates the Par complex to regulate Numb localization. Cell *135*, 161–173.

Xu, J., Wang, H., Liang, T., Cai, X., Rao, X., Huang, Z., and Sheng, G. (2012). Retinoic acid promotes neural conversion of mouse embryonic stem cells in adherent monoculture. Mol. Biol. Rep. *39*, 789–795.

Yao, Y., Shao, C., Jothianandan, D., Tcherepanov, A., Shouval, H., and Sacktor, T.C. (2013). Matching biochemical and functional efficacies confirm ZIP as a potent competitive inhibitor of PKMζ in neurons. Neuropharmacology *64*, 37–44.

Ying, Q.L., Wray, J., Nichols, J., Batlle-Morera, L., Doble, B., Woodgett, J., Cohen, P., and Smith, A. (2008). The ground state of embryonic stem cell self-renewal. Nature *453*, 519–523.

Zhou, P., Alfaro, J., Chang, E.H., Zhao, X., Porcionatto, M., and Segal, R.A. (2011). Numb links extracellular cues to intracellular polarity machinery to promote chemotaxis. Dev. Cell *20*, 610–622.